Opposing roles of cell death-inducing DFF45-like effector B and perilipin 2 in controlling hepatic VLDL lipidation[S]

Xuanhe Li,* Jing Ye,[†] Linkang Zhou,* Wei Gu,* Edward A. Fisher,[§,,††] and Peng Li[1,*]**

Tsinghua-Peking Center for Life Sciences,* School of Life Sciences, Tsinghua University, Beijing, China; Department of Pathology,[†] Fourth Military Medical University, Xi'an, Shaanxi, China; and Departments of Medicine (Cardiology)[§] and Cell Biology** and the Marc and Ruti Bell Program in Vascular Biology,[††] School of Medicine, New York University, New York, NY

Abstract Regulation of hepatic very low density lipoprotein (VLDL) assembly and maturation is crucial in controlling lipid homeostasis and in the development of metabolic disorders, including obesity, hepatic steatosis, and insulin resistance. Cideb, a member of cell death-inducing DFF45-like effector (CIDE) protein family, has been previously shown to promote VLDL lipidation and maturation. However, the precise subcellular location of Cideb-mediated VLDL lipidation and the factors modulating its activity remain elusive. In addition to its localization to endoplasmic reticulum (ER) and lipid droplets (LD), we observed that Cideb was also localized to the Golgi apparatus. Mature and lipid-rich VLDL particles did not accumulate in the Golgi apparatus in *Cideb*$^{-/-}$ livers. Interestingly, we observed that hepatic perilipin 2/adipose differentiation-related protein (ADRP) levels were markedly increased in *Cideb*$^{-/-}$ mice. Liver-specific knockdown of perilipin 2 in *Cideb*$^{-/-}$ mice resulted in the reduced accumulation of hepatic triglycerides (TAG), increased VLDL-TAG secretion, and the accumulation of mature TAG-rich VLDL in the Golgi apparatus. These data reveal that Cideb and perilipin 2 play opposing roles in controlling VLDL lipidation and hepatic lipid homeostasis.—Li, X., J. Ye, L. Zhou, W. Gu, E. A. Fisher, and P. Li. **Opposing roles of cell death-inducing DFF45-like effector B and perilipin 2 in controlling hepatic VLDL lipidation. *J. Lipid Res.* 2012.** 53: **1877–1889.**

Supplementary key words Cideb • very low density lipoprotein maturation • lipid droplet

Hepatic lipid homeostasis, including lipid storage and very low density lipoprotein (VLDL) assembly and secretion, is important for controlling the plasma levels of triglycerides (TAG) and cholesterol and for the development of metabolic disorders, including obesity, diabetes, and hepatic steatosis. It is believed that VLDL assembly and maturation involves two steps (1, 2). The first step is the formation of lipid-poor pre-VLDL particles involving the cotranslational lipidation of apolipoprotein B (apoB) with a few lipids, aided by microsomal triglyceride transfer protein (MTP) (3, 4). The second step is the transfer of large quantities of lipids, likely from TAG-rich lipid droplets (LD), to the pre-VLDL particles, converting the pre-VLDL particles into lipid-rich, mature VLDL particles (2–5). Thus far, the subcellular site of the addition of bulk lipids to pre-VLDL particles, the source of the lipids, and the factors promoting VLDL lipidation remain unclear. The endoplasmic reticulum (ER) has been suggested as the VLDL lipidation site because the majority of TAG is synthesized in the ER, and apoB-100 has been shown to be localized to the ER membrane (2, 6, 7). Others believe that the pre-VLDL particles are assembled in the ER and then exit, with the final VLDL lipidation and maturation occurring primarily within the Golgi apparatus or post-ER compartments (8–11). For example, the biochemical separation of the lipoprotein particles from McA-RH7777 cells indicated that mature VLDL particles accumulate in the Golgi but not in the ER fractions (11, 12). In addition, the late addition of bulk lipids to pre-VLDL particles is independent of both MTP activity and new triglyceride synthesis (12, 13).

The availability of neutral lipids and the capacity to transfer TAG to pre-VLDL particles are crucial for VLDL lipidation and maturation. The LD, a subcellular organelle,

This work was supported by National Natural Science Foundation of China Grant 31030038 (to P.L.), National High Technology Research and Development Grant 2010AA023002 from the Ministry of Science and Technology of China, and National Institutes of Health Grant HL-58541 (to E.A.F.). Its contents are solely the responsibility of the authors and do not necessarily represent the official views of the National Institutes of Health.

Manuscript received 19 March 2012 and in revised form 31 May 2012.

Published, JLR Papers in Press, June 1, 2012
DOI 10.1194/jlr.M026591

Abbreviations: ADRP, adipose differentiation-related protein; CIDE, cell death-inducing DFF45-like effector; CNX, calnexin; ER, endoplasmic reticulum; LD, lipid droplet; MTP, microsomal triglyceride transfer protein; OA, oleic acid; TAG, triglyceride; Tip47, tail interacting protein of 47 kDa.

[1]To whom correspondence should be addressed.
e-mail: li-peng@mail.tsinghua.edu.cn

[S]The online version of this article (available at http://www.jlr.org) contains supplementary data in the form of one table and three figures.

is the main site of neutral lipid storage in all cell types (14, 15). Recently, the LD has been recognized as a dynamic and functionally active organelle that regulates protein trafficking, viral assembly, and insulin sensitivity (16–20). Two types of LDs, cytosolic LDs and ER-associated lumenal LDs, have been identified (21, 22). LDs have been demonstrated to be in close proximity to the ER-derived membrane in hepatocytes with downregulated perilipin 2/adipose differentiation-related protein (ADRP) (23) or stuck in the ER membrane by tight binding to lipidated apoB-100 (24). It is generally believed that cytosolic LDs represent a major source of lipids for VLDL maturation (25, 26). However, the molecular mechanism by which TAG is transferred from cytosolic LDs to pre-VLDL particles remains a subject of intense discussion and debate. It has been proposed that TAG can be transferred from LDs in the ER lumen to pre-VLDL particles through their direct fusion (4, 13). Alternatively, TAG from cytosolic LDs can be hydrolyzed to yield free fatty acids (FFA) that are then reesterified on the lumenal side of secretory pathway organelles, such as the ER and the Golgi apparatus, to form a special form of lumenal LDs that can be incorporated into nascent VLDL particles (27–30).

It remains to be determined whether TAG from cytosolic LDs can be directly transferred to pre-VLDL particles to form lipid-rich VLDL particles. One potential factor in this process is perilipin 2, a member of the PAT protein family. Perilipin 2 is associated with LDs and has been shown to regulate VLDL assembly and LD morphology in hepatocytes (31–33). *Perilipin 2* deficiency protects mice from the development of hepatic steatosis by reducing TAG storage and promoting VLDL assembly and secretion (33–35). *Perilipin 2* and *ApoE* double-deficient mice exhibit impaired foam cell formation and resistance to the development of atherosclerosis (36). The downregulation of perilipin 2 and perilipin 3/tail interacting protein of 47 kDa (Tip47) in AML12 cells increases lipolysis by enhancing the recruitment of adipose triglyceride lipase (ATGL) to the LD surface (18). In contrast, the overexpression of perilipin 2 inhibits the association of ATGL with LDs, reduces lipolysis (37), stimulates lipid biosynthesis, and inhibits fatty acid β-oxidation (38). However, the exact mechanism by which perilipin 2 controls VLDL lipidation and lipid storage remains unknown.

The cell death-inducing DFF45-like effector (CIDE) proteins, including Cidea, Cideb, and Fsp27 (Cidec in human), are crucial regulators of lipid metabolism and play important roles in the development of metabolic disorders, including obesity, insulin resistance, and hepatic steatosis (39–44). Cideb is expressed at high levels in the liver, and its deficiency results in higher energy expenditure, reduced plasma TAG levels (45) and altered expression of genes in various metabolic and signaling networks (46). Furthermore, Cideb is localized to the LD and ER and facilitates VLDL lipidation and maturation, possibly through its interaction with apoB (47). Here, we demonstrate that, in addition to its subcellular localization on the LDs and ER, Cideb was associated with the Golgi apparatus, and Cideb deficiency led to the decreased accumulation of mature VLDL in this organelle. Interestingly, we found that perilipin 2 expression was markedly increased in the livers of *Cideb*$^{-/-}$ mice. Knocking down perilipin 2 in the livers of *Cideb*$^{-/-}$ mice resulted in increased lipid storage and enhanced VLDL-TAG secretion and accumulation of lipid-rich mature VLDL particles in the Golgi, rescuing the phenotypes caused by *Cideb* deficiency.

MATERIALS AND METHODS

Materials

All chemicals were purchased from Sigma-Aldrich (USA) unless otherwise stated. The rabbit anti-mouse Cideb antibody was used as previously described (45). The following antibodies were purchased from the indicated companies: guinea pig anti-perilipin 2 antibody (Fitzgerald Industries, USA), goat anti-apoB antibody (AB742, Chemicon, USA), mouse anti-MTP and mouse anti-GM130 antibodies (BD Biosciences, USA), mouse anti-Golgi 58K protein (p58K), mouse anti-β-actin and rabbit anti-calnexin (CNX) antibodies (Sigma-Aldrich, USA) and rat anti-GRP94 antibody (Santa Cruz Biotechnology, USA). The mouse anti-perilipin 5 antibody was a gift from Jing Ye's lab (Department of Pathology, Fourth Military Medical University). The protease inhibitor mixture tablets were purchased from Roche Diagnostics (Switzerland). The [^{3}H]oleic acids were purchased from PerkinElmer (USA).

Animals

Cideb$^{-/-}$ mice were generated and maintained as previously described (45). *Cideb*$^{-/-}$ mice and wild-type C57BL/6J mice were housed in an environmentally controlled animal facility of the Center of Biomedical Analysis, Tsinghua University, Beijing, China. Mice had access to food and autoclaved water ad libitum. Twelve-week-old male mice were used in the studies. The mice were handled according to the Responsible Care and Use of Laboratory Animals guideline set by Tsinghua University, and the experimental protocols were approved by the animal ethics committee of Tsinghua University.

Isolation and culture of primary hepatocytes

Hepatocytes were isolated from livers of 12-week-old mice as previously described (48). The mice were anesthetized with 1% Pelltobarbitalum Natricum (AMRESCO, USA) and dissected. The livers were perfused through the portal veins to remove the blood, and the perfusion was continued until the livers became soft. The livers were immediately removed, cut into pieces, and mixed with a collagenase solution until the hepatocytes were dispersed. The hepatocytes were filtered to remove tissue debris and washed three times with cold Dulbecco's modified Eagle's medium (DMEM, Invitrogen, USA). The isolated hepatocytes were suspended in DMEM containing 10% fetal bovine serum (FBS, Invitrogen, USA) and seeded at 1×10^6 cells/dish in 6 cm dishes. Cells were maintained in 5% CO_2 at 37°C.

Subcellular fractionation and analysis of microsomal lumenal TAG contents

Subcellular fractionation was performed essentially as previously described (11). Livers were removed and rapidly homogenized with a loose-fitted Dounce homogenizer in 5 ml of ice-cold solution containing 10 mM Hepes, pH 7.4, 150 mM sucrose, 0.5 mM DTT, and 1× EDTA-free protease inhibitors. The homogenates were centrifuged at 1,900 *g* for 10 min at 4°C, and the supernatants were centrifuged at 100,000 *g* for 90 min at 4°C in a Beckman SW60 rotor. The LD fraction floated on the top was

collected. The pellets were resuspended in 2.3 ml of an 8.58% sucrose solution and loaded on top of a sucrose density gradient containing the following layers (from the bottom): 56% (0.46 ml), 50% (0.92 ml), 45% (1.38 ml), 40% (2.3 ml), 35% (2.3 ml), 30% (1.38 ml), and 20% (0.46 ml) sucrose. After ultracentrifugation at 39,000 rpm for 18 h at 4°C in a Beckman SW41 rotor, 12 fractions were unloaded from top to bottom of each centrifuge tube. The distribution patterns of the subcellular compartment markers were determined by Western blotting (ER marker: CNX, GRP94, MTP; Golgi marker: GM130, p58), and the intensities of the bands were determined semiquantitatively using Bio-Rad Quantity One software.

The Golgi or ER fractions were combined and centrifuged at 100,000 *g* for 90 min at 4°C. The microsome pellets were resuspended in lysis buffer (20 mM Tris-HCl, 150 mM NaCl, 1 mM EDTA, 1 mM EGTA, 1% Triton-X100, and protease inhibitors, at pH 7.4), and the TAG levels were measured using the Serum Triglyceride Determination Kit (Sigma TR0100).

Sucrose gradient separation of apoB-containing lipoproteins from the isolated ER and Golgi lumenal contents

Separation of the lumenal apoB-containing lipoproteins was performed as described (11). The lumenal contents were released from microsomes by treatment with 0.1 M sodium carbonate (pH 11) and deoxycholic acid (0.025%) for 25 min at room temperature. BSA was added to a final concentration of 5 mg/ml, and the samples were centrifuged at 50,000 rpm in a Beckman SW60 rotor for 1 h at 4°C. The lumenal contents (supernatant) were adjusted to pH 7.4 by the addition of 10% acetic acid and adjusted to a sucrose concentration of 12.5% (w/v). The adjusted supernatants were placed on the top of a step gradient consisting of 1.9 ml of 49% sucrose and 1.9 ml of 20% sucrose. Next, 2.8 ml of phosphate-buffered saline (PBS) was layered on the top of the supernatants. All solutions contained protease inhibitors. After centrifugation at 35,000 rpm for 65 h at 10°C in a Beckman SW41 rotor, 12 fractions (0.95 ml each) with densities ranging from 1.0 to 1.125 g/ml were collected from the top of the tube. ApoB was immunoprecipitated from each fraction. The density of each fraction was determined as the ratio of the weight of a 1 ml aliquot to the weight of a 1 ml aliquot of water. The apoB distribution patterns in the Golgi and ER lumens were determined by immunoblotting, and the intensities of the bands were determined semiquantitatively using Bio-Rad Quantity One software.

Western blots

Livers were homogenized in lysis buffer (20 mM Tris-HCl, 150 mM NaCl, 1 mM EDTA, 1 mM EGTA, 1% Triton-X100, and protease inhibitors, at pH 7.4) and centrifuged to discard the cell debris. The protein concentrations were determined using a Bio-Rad kit (USA). Equivalent amounts of protein homogenate were resolved by SDS-PAGE, transferred to a polyvinylidene difluoride (PVDF) membrane, and probed with specific antibodies for visualization.

RNA extraction and semiquantitative real-time PCR

Total RNA was isolated from mice livers with TRIzol (Invitrogen, USA). First-strand cDNA synthesis was performed using the Superscript III RT kit and oligo-dT primers (Invitrogen, USA). Semiquantitative real-time PCR (RT-PCR) reactions were performed using the SYBR Green PCR system (Applied Biosystems, USA) in an ABI 7500 thermal cycler (Applied Biosystems, USA). β-actin was used as a reference gene. The primers for real-time PCR are described in supplementary Table I.

Liver lipid extraction and TLC assay

The total lipids were extracted from livers as previously described (49). The livers were homogenized in PBS buffer containing protease inhibitors. The homogenates were rapidly mixed with a chloroform / methanol (2:1) solution by vortexing and centrifuged at 250 *g* for 10 min to separate the phases. The lower lipid-containing phase was carefully aspirated and dried in a 70°C metal bath with nitrogen steam. The dried lipids were reconstituted in methylbenzene and loaded onto a TLC plate. The lipids were separated in a hexane / diethyl ether / acetic acid (70:30:1, v/v) solution. The TLC plates were sprayed with 10% $CuSO_4$ in 10% phosphoric acid and developed by drying in a 120°C oven.

Analysis of plasma TAG contents

After the mice fasted for 12 h, blood was collected from the orbital plexus, and serum was isolated after centrifugation. The serum TAG levels were determined using the Serum Triglyceride Determination Kit (Sigma TR0100).

TAG synthesis and fatty acid β-oxidation

Fifty thousand viable hepatocytes per well were cultured in 6-well plates for 12 h in DMEM containing 10% FBS. The hepatocyte monolayers were washed twice with PBS buffer before being tested for TAG synthesis and fatty acid β-oxidation. The reactions were carried out in triplicate (2 ml per well), each containing [^{3}H]oleic acid (1 μCi/well) with 22 μM unlabeled oleic acid and 0.5 mg/ml fatty acid-free BSA in PBS. After incubation at 37°C for 2 h, the monolayers were scraped into centrifuge tubes in 2 ml PBS, and 8 ml hexane/isopropanol (3:2) was added. After vigorously mixing, the tubes were centrifuged at 3,000 *g* for 5 min. The upper phase, containing the lipids, was transferred to vials and dried under nitrogen steam. The TAG was separated on a TLC plate and collected. Five milliliters of scintillation solution were added, and the radioactivity was measured. The protein pellets were dried and dissolved in 1 ml 0.2 M KOH solution overnight. The protein content was determined using the Bradford method.

For the measurement of fatty acid β-oxidation, the reaction medium was transferred to glass tubes after incubation at 37°C for 2 h or 4 h, and 8 ml of methanol/chloroform (2:1) was added. After vigorously mixing, the mixtures were centrifuged at 3,000 *g* for 5 min, the aqueous phase containing ^3H_2O was transferred to a new tube, and the radioactivity was measured.

Analysis of in vivo VLDL-TAG and apoB secretion

The rate of VLDL secretion was determined by blocking the catabolism and clearance of VLDL with Triton WR-1339 (50). Mice were injected with 500 mg/kg body weight of Triton WR-1339 (in PBS) by tail-vein injection after 12 h of fasting. One hundred microliters of blood was drawn from the retro-orbital plexus at 1 h intervals after the injection, and the serum TAG concentrations were measured using the Serum Triglyceride Determination Kit (Sigma TR0100). Levels of apoB-100 and apoB-48 were visualized by Western blot analysis, and the intensities of the bands were semiquantitatively determined using Bio-Rad Quantity One software.

Preparation of the recombinant adenovirus and tail-vein injection

The recombinant adenoviruses carrying perilipin 2 shRNA or control shRNA were constructed using the AdEasy-1 System (Stratagene). The perilipin 2-targeting shRNA sequence was as follows: 5′- GAATATGCACAGTGCCAAC -3′. The viruses were packaged and amplified in AD293 cells and purified by CsCl density gradient ultracentrifugation, dialyzed against PBS supplemented

with 15% glycerol, and stored at −80°C. The adenoviruses were injected via the tail vein at a dosage of 1×10^{12} pfu/mouse. The plasma and liver TAG were examined 6 days after viral injection.

Immunofluorescent staining

Hepatocytes were cultured for 24 h and fixed with 4% paraformaldehyde for 1 h at room temperature. Bodipy 493/503 (Molecular Probes, USA) was used for neutral lipid staining. The nuclei were stained with Hoechst (Molecular Probes, USA). The sections were observed using a Zeiss 200M inverted microscope, and images were collected with an AxioCam MRm camera and AxioVision software.

Histology

The livers were excised and fixed in 10% formalin buffer. The fixed specimens were sectioned and stained with Oil Red O. Isolated hepatocytes were fixed in 10% buffered formalin and stained with Oil Red O.

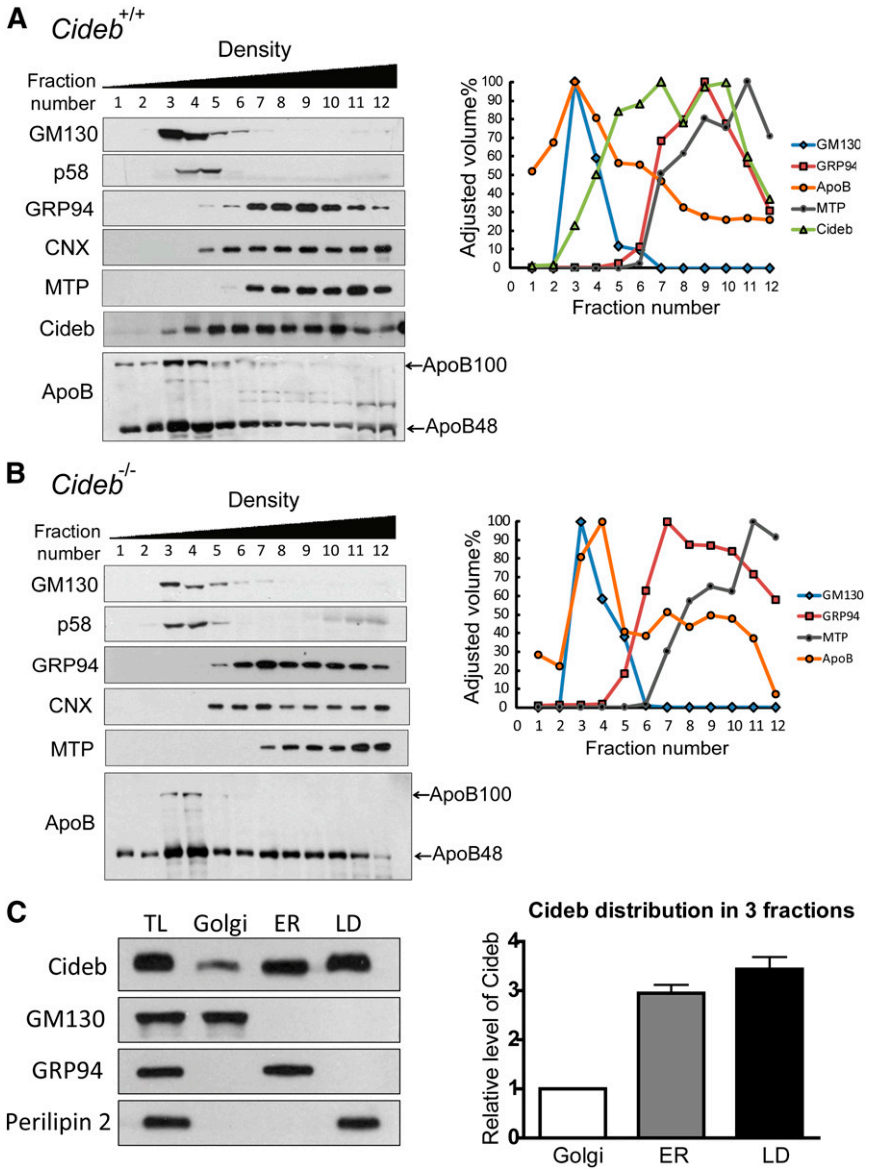

Fig. 1. Distribution patterns of Cideb, perilipin 2, ApoB, and marker proteins in the Golgi and ER fractions. (A, B) Biochemical fractionation of liver microsomes was performed by sucrose density gradient ultracentrifugation using wild-type (+/+) (A) and *Cideb*$^{-/-}$ (−/−) (B) mice. The presence of specific proteins in each fraction was determined by Western blot analysis with various antibodies (left panels). GM130 and p58 represent Golgi markers. GRP94, CNX, and MTP are ER-specific markers. The intensities of the positive bands on the immunoblots were determined semiquantitatively using Bio-Rad Quantity One software and plotted as the percentage of the maximum value, in which 100% corresponds to the highest value (right panels). (C) Comparison of the relative levels of Cideb in the Golgi, ER, and LD compartments. The Golgi, ER, and LD fractions were collected after further ultracentrifugation and normalized to 600 μl. Three microliters of each fraction was loaded for immunoblot analysis (left panel). GM130, a Golgi marker; GRP94, an ER marker; perilipin 2, a LD marker. The intensities of the Cideb bands on the immunoblots were determined semiquantitatively using Bio-Rad Quantity One software, and the abundances of Cideb in the ER and LDs were compared with that in the Golgi (right panel). The experiment was repeated three times.

Statistical analysis

The data are presented as means ± SEM. Student *t*-tests were used to determine significant differences between treatment groups. $P < 0.05$ was considered statistically significant.

RESULTS

Cideb is localized to the Golgi apparatus

To further evaluate the role of Cideb in regulating VLDL lipidation and maturation, we assessed the presence of Cideb in the Golgi apparatus, which plays an important role in VLDL lipidation and maturation. We first isolated ER and Golgi membrane fractions from mice livers using a sucrose density gradient centrifugation approach (11). The fractions were loaded according to their density, and the Golgi membranes were enriched in fractions 3–5 based on the detection of two Golgi-specific markers, 130 kDa *cis*-Golgi matrix protein (GM130) and Golgi 58K protein (p58), in these fractions. Higher levels of glucose-regulated protein 94 kDa (GRP94), CNX, and MTP, three ER-specific markers, were detected in fractions 6–12, suggesting ER enrichment in these fractions. Interestingly, Cideb exhibited a broad distribution pattern, and this protein was detected in fractions 3–12, spanning both the Golgi and ER fractions (**Fig. 1A**). As a LD-associated protein, perilipin 2 was only detected in the LD but not in the ER or Golgi-enriched fractions. Cideb was also detected in the LD fraction. Consistent with previous observations that VLDL lipidation and maturation occurs in the Golgi apparatus (11, 12), apoB-100 and apoB-48 were mainly detected in the low-density fractions (fractions 1–4), with the highest levels present in the Golgi-enriched fractions (fractions 3–4). These data indicate that, in addition to its ER and LD association, Cideb is associated with the Golgi apparatus. Subcellular fractionation of liver tissues from *Cideb*$^{-/-}$ mice showed no difference in the distribution of various markers in the appropriate fractions (Fig. 1B). Interestingly, we observed a slight but consistent shift of the apoB peak from fraction 3 to fraction 4, which may correlate with the accumulation of less lipidated VLDL particles in the livers of *Cideb*$^{-/-}$ mice. When the relative levels of Cideb in the Golgi, ER, and LD fractions were normalized and compared, we observed that the amounts of Cideb in the ER and LDs were approximately 3- and 3.5-fold higher, respectively, than those in Golgi apparatus (Fig. 1C).

Reduced VLDL accumulation in the Golgi of *Cideb*$^{-/-}$ liver tissue

To further evaluate the role of Cideb in VLDL lipidation and maturation in the Golgi, we isolated the Golgi and ER microsomal fractions from the livers of wild-type and *Cideb*$^{-/-}$ mice and measured the amount of TAG in the Golgi and ER, respectively. In wild-type liver tissue, the amount of TAG in the Golgi was 2-fold higher than that in the ER, consistent with the role of the Golgi in VLDL lipidation. Interestingly, we observed an approximately 50% reduction in the amount of TAG in the Golgi fraction from *Cideb*$^{-/-}$ livers compared with livers from wild-type mice (57.30 ± 3.25 versus 115.60 ± 5.46 mg/g protein, $P < 0.001$, **Fig. 2A**). In contrast, the amount of TAG in the ER fraction was similar between the wild-type and *Cideb*$^{-/-}$ livers (50.61 ± 4.58 versus 40.32 ± 5.16 mg/g protein, Fig. 2A). Therefore, significantly fewer mature and lipid-rich VLDL particles accumulated in the Golgi apparatus in *Cideb*$^{-/-}$ livers.

Next, we isolated the Golgi and ER microsomes from the livers of wild-type and *Cideb*$^{-/-}$ mice and treated them with sodium carbonate and deoxycholate to release the apoB-containing lipoproteins (11). The released lipoproteins from the ER and Golgi were separated by sucrose density gradient centrifugation, and the apoB in individual density fractions was immunoprecipitated. The presence of apoB in each fraction was evaluated by Western blot analysis. As shown in Fig. 2B, the Golgi microsomes from the livers of wild-type mice contained lipoproteins with densities ranging from 1.0 to 1.053, representing VLDL and IDL/LDL particles. However, the lipoproteins isolated from the Golgi of *Cideb*$^{-/-}$ livers exhibited densities

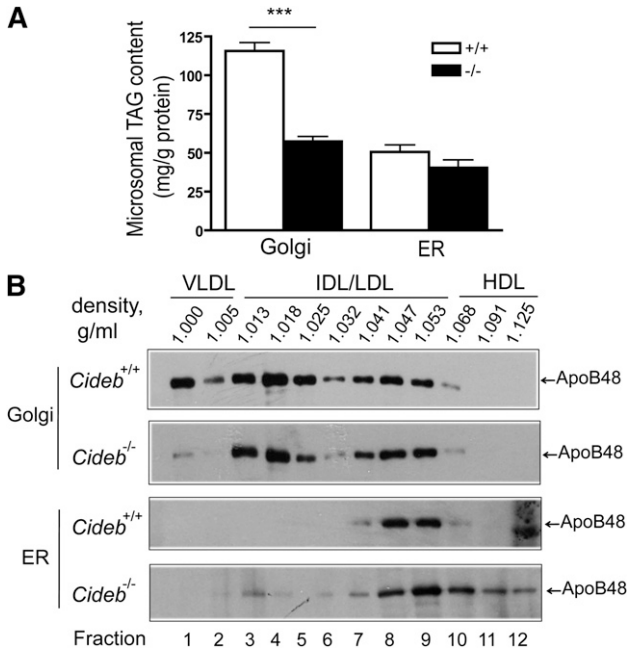

Fig. 2. Reduced levels of mature VLDL in the liver Golgi fractions of *Cideb*$^{-/-}$ mice. (A) Hepatic microsomal TAG levels from wild-type (+/+) and *Cideb*$^{-/-}$ (–/–) mice (n = 5 each). The fractions (3–5 for the Golgi and 6–12 for the ER from Fig. 1A) were combined, collected by ultracentrifugation, and resuspended in lysis buffer. The TAG levels contained were measured using the Serum Triglyceride Determination Kit (Sigma TR0100). ***$P < 0.001$. Data are the means ± SEM. (B) The distribution of apoB-containing lipoproteins in the Golgi and ER fractions from *Cideb*$^{-/-}$ and wild-type mice. The Golgi (3–5) and ER (6–12) fractions were incubated with sodium carbonate and deoxycholate to release the lipoprotein particles, which were then subjected to sucrose density gradient centrifugation to separate the apoB-containing lipoproteins. ApoB was immunoprecipitated from each fraction, separated by SDS-PAGE and assessed by fluorography. The results shown are representative of three independent experiments. The labels at the top are the measured densities, indicating the expected distributions of the lipoproteins. HDL, high-density lipoprotein; IDL/LDL, intermediate/low-density lipoprotein.

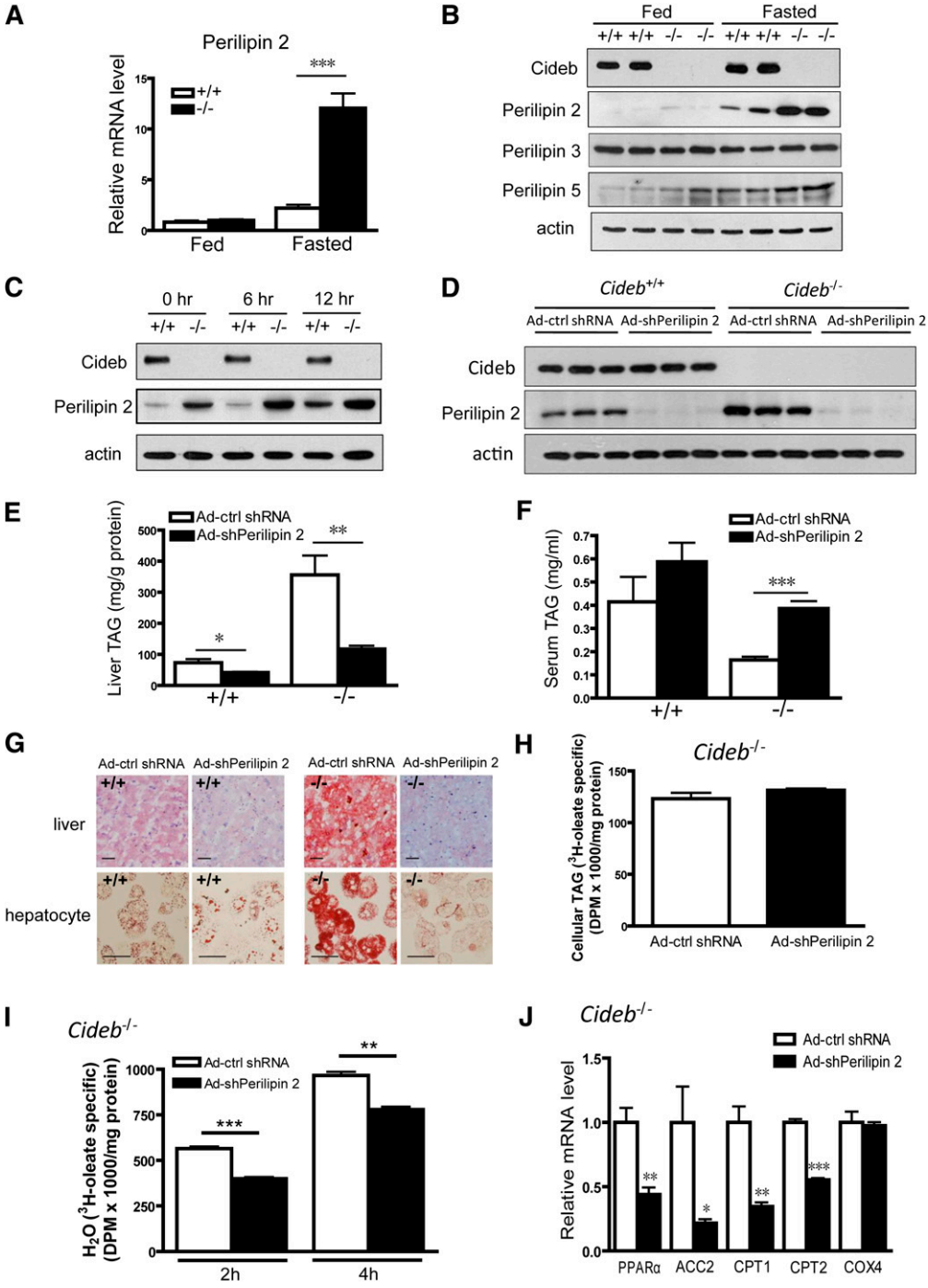

Fig. 3. Knockdown of perilipin 2 in the livers of *Cideb*$^{-/-}$ mice results in decreased hepatic TAG accumulation. (A) Relative mRNA levels of perilipin 2 in the livers of 3-month-old wild-type (+/+) and *Cideb*$^{-/-}$ (−/−) mice (n = 5 each) under fed or fasting conditions. ***$P < 0.001$. Data are the means ± SEM. (B) Western blot showing increased perilipin 2 and perilipin 5 protein levels in the livers of *Cideb*$^{-/-}$ (−/−) mice under fasting conditions and no change in perilipin 3 levels in the absence of Cideb under either condition. The samples depicted are representative of four samples for each group. (C) Western blot showing increased perilipin 2 protein levels in *Cideb*$^{-/-}$ (−/−) hepatocytes in the presence or absence of 400 μm OA for the indicated duration. The samples depicted are representative of four independent experiments. (D) Perilipin 2 was knocked down in the livers of wild-type and *Cideb*$^{-/-}$ mice. Perilipin 2 shRNA was packaged into adenovirus (Ad-shPerilipin 2), and scrambled shRNA adenovirus was used as a negative control (Ad-ctrl shRNA). The viruses were introduced into 3-month-old *Cideb*$^{-/-}$ mice (n = 5 each) by tail-vein injection. The mice were sacrificed, and the livers were collected one week after injection. The samples depicted are representative of five samples for each group. (E) Knockdown of perilipin 2 decreased hepatic TAG levels in both wild-type (+/+) and *Cideb*$^{-/-}$ (−/−) mice (n = 5 each). *$P < 0.05$, **$P < 0.01$. Data are the means ± SEM. (F) Knockdown of perilipin 2 increased the plasma TAG levels in *Cideb*$^{-/-}$ (−/−) mice (n = 5 each). The serum was collected 12 h after fasting. ***$P < 0.001$. Data are the means ± SEM. (G) Representative photomicrographs of liver sections

ranging from 1.013 to 1.053 (IDL/LDL lipoproteins) and consisted of significantly fewer VLDL particles. In contrast, the ER fractions from the livers of both wild-type and *Cideb*$^{-/-}$ mice contained apoB-containing lipoproteins with densities of 1.041–1.053 (i.e., LDL range) but no VLDL or IDL density particles. In addition, the ER fractions from the livers of *Cideb*$^{-/-}$ mice contained a unique high-density lipoprotein species. These data not only confirm our previous observation that Cideb promotes VLDL lipidation and maturation but also further suggest that Cideb may mediate VLDL lipidation in the Golgi apparatus.

Increased perilipin 2 expression in the livers of *Cideb*$^{-/-}$ mice

As Cideb is a LD-associated protein, we hypothesized that other LD-associated proteins may influence Cideb-mediated VLDL lipidation and maturation. To identify potential factors in the Cideb-mediated VLDL lipidation pathway, we assessed the expression levels of several LD-associated proteins, including PAT family proteins (perilipin 1, perilipin 2, perilipin 3, and perilipin 5) and the other two CIDE family proteins (Cidea and Fsp27) in the livers of *Cideb*$^{-/-}$ mice. The perilipin 1, Cidea, and Fsp27 proteins were not detected in the livers of wild-type and *Cideb*$^{-/-}$ mice (data not shown). Interestingly, we observed a marked increase in the expression of perilipin 2 at both the mRNA and protein levels in the livers of *Cideb*$^{-/-}$ mice under fasting conditions ($P < 0.001$, **Fig. 3A**, B). Hepatic levels of perilipin 5 were slightly increased in *Cideb*-deficient mice (Fig. 3B). However, the hepatic levels of perilipin 3 were similar between wild-type and *Cideb*$^{-/-}$ mice under both fed and fasting conditions (Fig. 3B). Markedly increased perilipin 2 levels and slightly higher levels of perilipin 3 and perilipin 5 were also observed in the LD fractions of *Cideb*$^{-/-}$ mice compared with that of wild-type mice (supplementary Fig. I-A). In addition, the protein levels of perilipin 2 were significantly higher in isolated *Cideb*$^{-/-}$ hepatocytes treated with oleic acid (OA) (Fig. 3C). These data indicate that the levels of perilipin 2 were significantly upregulated in the livers of *Cideb*$^{-/-}$ mice.

Reduced TAG accumulation in the livers of perilipin 2 knockdown and *Cideb*$^{-/-}$ mice

To evaluate the role of perilipin 2 in modulating Cideb-mediated VLDL lipidation, we knocked down perilipin 2 expression in the livers of wild-type and *Cideb*$^{-/-}$ mice using a targeted adenoviral system. As shown in Fig. 3D, adenoviruses containing shRNA against perilipin 2 (Ad-shPerilipin 2) effectively reduced hepatic perilipin 2 expression compared with adenoviruses containing scrambled shRNA (Ad-ctrl shRNA) in both wild-type and *Cideb*$^{-/-}$ mice. The knockdown of perilipin 2 did not change the levels of perilipin 3 but slightly reduced the total levels of perilipin 5 in the livers of both wild-type and *Cideb*$^{-/-}$ mice (supplementary Fig. I-B). However, the amounts of LD-associated perilipin 3 and perilipin 5 were significantly increased in *Cideb*$^{-/-}$ livers with a liver-specific knockdown of perilipin 2 (supplementary Fig. I-C). The knockdown of perilipin 2 in the livers of wild-type mice moderately reduced hepatic TAG accumulation (41.98 ± 2.52 versus 73.43 ± 11.96 mg/g protein for perilipin 2 knockdown and control, respectively, $P < 0.05$). Intriguingly, perilipin 2 knockdown markedly reduced hepatic TAG levels in the livers of *Cideb*$^{-/-}$ mice (117.50 ± 10.66 versus 356.00 ± 62.13 mg/g protein for the perilipin 2 knockdown and control, respectively, $P < 0.01$, Fig. 3E). The decreased TAG accumulation was also evident in isolated *Cideb*$^{-/-}$ hepatocytes that were stained with Oil Red O (Fig. 3G). The decreased hepatic TAG levels in the perilipin 2 knockdown and *Cideb*$^{-/-}$ hepatocytes were not due to the downregulation of TAG synthesis, because the hepatic TAG synthesis rate was not changed (Fig. 3H) and the mRNA levels of lipogenic genes involved in fatty acid synthesis [acetyl-CoA carboxylase 1 (ACC1), fatty acid synthase (FAS), and stearol-CoA desaturase 1 (SCD1)] and TAG synthesis [diacylglycerol O-acyltransferase 1 (DGAT1) and diacylglycerol O-acyltransferase 2 (DGAT2)] were similar between the perilipin 2-knockdown and control mice (data not shown). The reduced hepatic TAG levels were not due to the increased fatty acid β-oxidation, as the rate of fatty acid β-oxidation in *Cideb*$^{-/-}$ hepatocytes with perilipin 2 knockdown was significantly reduced (Fig. 3I). Consistent with a decreased rate of fatty acid oxidation, the expression levels of genes involved in fatty acid β-oxidation, including peroxisome proliferator-activated receptor α (PPARα), acetyl-CoA carboxylase 2 (ACC2), carnitine-palmitoyl transferase 1 (CPT1), carnitine-palmitoyl transferase 2 (CPT2), and cytochrome c oxidase subunit IV (COX4), were reduced (Fig. 3J). In contrast to the reduced hepatic TAG levels, the plasma levels of TAG were significantly increased in the *Cideb*$^{-/-}$ mice with liver-specific knockdown of perilipin 2 (0.386 ± 0.032 versus 0.164 ± 0.014 mg/ml for the perilipin 2 knockdown and control, respectively, $P < 0.001$, Fig. 3F). These data indicate that perilipin 2 knockdown in the livers of *Cideb*$^{-/-}$ mice leads to reduced hepatic TAG accumulation and increased plasma TAG levels.

(upper panel) and isolated hepatocytes (lower panel) from *Cideb*$^{-/-}$ (−/−) and wild-type (+/+) mice stained with Oil Red O after treatment with Ad-shPerilipin 2 and control virus (Ad-ctrl shRNA). Scale bars, 50 μm. (H) Rates of TAG synthesis in *Cideb*$^{-/-}$ hepatocytes. Hepatocytes with perilipin 2 knockdown and control cells (n = 3 each) were incubated with radiolabeled [^{3}H]oleic acid for 2 h. The TAG in the hepatocytes was extracted and evaluated by TLC. Data are the means ± SEM. (I) Decreased fatty acid β-oxidation rate in *Cideb*$^{-/-}$ hepatocytes with perilipin 2 knockdown compared with control cells. The hepatocytes (n = 3 each) were incubated with radiolabeled [^{3}H]oleic acid for 2 h or 4 h. The ^3H_2O released into medium was extracted and evaluated. Data are the means ± SEM. $^{**}P < 0.01$, $^{***}P < 0.001$. (J) Relative mRNA levels of PPARα, ACC2, CPT1, CPT2, and COX4 in the livers of *Cideb*$^{-/-}$ mice treated with Ad-shPerilipin 2 or Ad-ctrl shRNA (n = 5 each). The mice were fasted for 12 h. $^{*}P < 0.05$, $^{**}P < 0.01$, $^{***}P < 0.001$.

Increased VLDL-TAG secretion in *Cideb*$^{-/-}$ mice with liver-specific knockdown of perilipin 2

The reduced hepatic TAG accumulation and increased plasma TAG levels in *Cideb*$^{-/-}$ mice with liver-specific knockdown of perilipin 2 suggest that hepatic TAG secretion might be increased. To test this in vivo, we injected the animals with Triton-WR1339 to block VLDL catabolism and clearance and measured the plasma TAG levels at various time points after injection. As shown in **Fig. 4A**, the VLDL-TAG secretion rate was significantly lower in *Cideb*$^{-/-}$ mice compared with wild-type mice. When perilipin 2 was knocked down in the *Cideb*$^{-/-}$ mice, the VLDL-TAG secretion rate was dramatically increased and reached the levels observed in wild-type mice, indicating that knocking down perilipin 2 rescued the VLDL-TAG secretion defect in *Cideb*$^{-/-}$ mice. The VLDL-TAG secretion was also markedly increased in wild-type mice with hepatic perilipin 2 knockdown. In addition, the plasma collected from *Cideb*$^{-/-}$

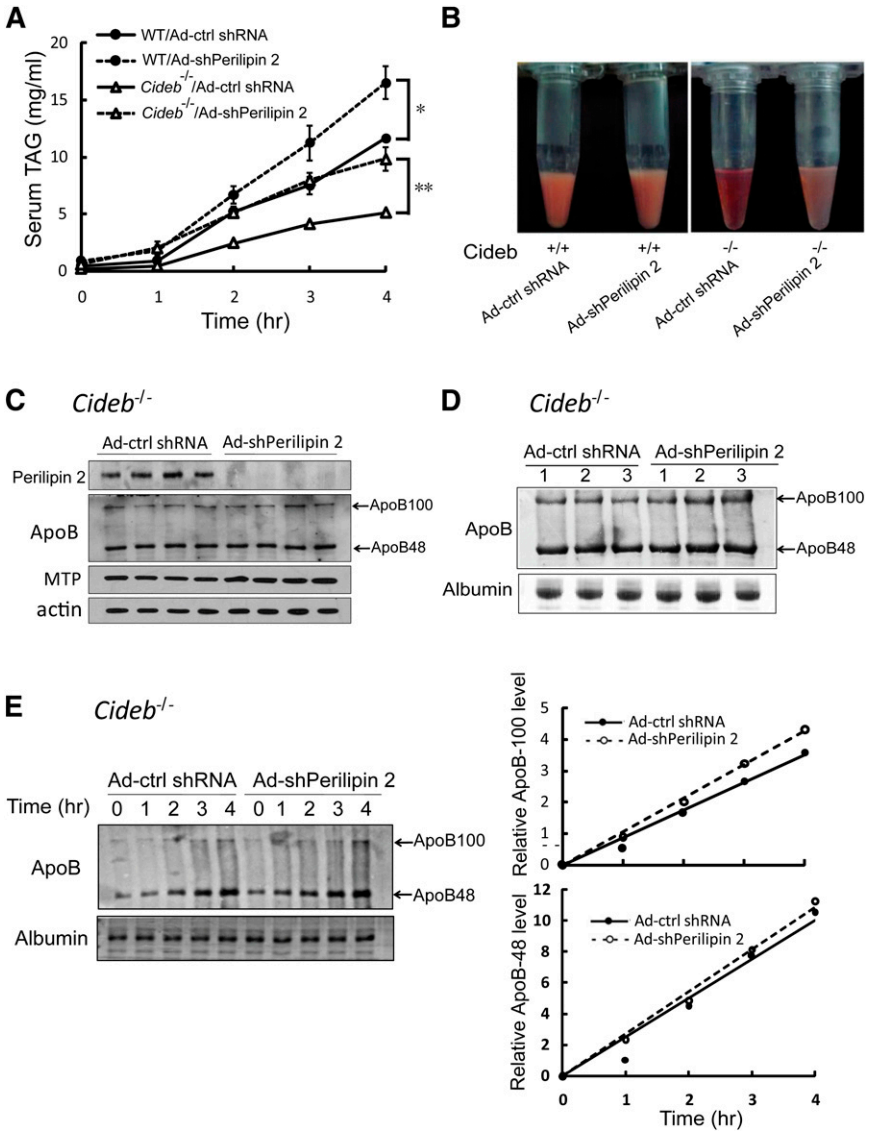

Fig. 4. Liver-specific knockdown of perilipin 2 increases VLDL-TG secretion in *Cideb*$^{-/-}$ mice without affecting apoB synthesis and secretion. (A) Knockdown of perilipin 2 led to significant increases in VLDL-TAG secretion in wild-type and *Cideb*$^{-/-}$ mice. After treatment with Ad-shPerilipin 2 or Ad-ctrl shRNA for a week, the *Cideb*$^{-/-}$ and wild-type mice were fasted for 12 h and injected with 500 mg/kg body weight Triton WR-1339. Blood samples were collected at the indicated time points after Triton WR-1339 injection (n = 4). *$P < 0.05$, **$P < 0.01$, ***$P < 0.001$. Data are the means ± SEM. (B) Representative photographs of the plasma samples of four samples from each group treated with Triton WR-1339 for 4 h. (C) Levels of liver apoB-100/apoB-48 and MTP in *Cideb*$^{-/-}$ mice treated with Ad-shPerilipin 2 and Ad-ctrl shRNA. (D) Levels of plasma apoB-100/apoB-48 in *Cideb*$^{-/-}$ mice treated with Ad-shPerilipin 2 and Ad-ctrl shRNA. Serum was collected 12 h after fasting. Albumin stained with Coomassie Brilliant Blue G-250 was used as a loading control. (E) The rates of apoB-100/apoB-48 secretion in *Cideb*$^{-/-}$ mice with or without perilipin 2 knockdown were similar. The mice were injected with Triton WR-1339 after 12 h of fasting, and blood was collected at the indicated durations. Levels of plasma apoB-100/apoB-48 were visualized by immunoblotting (left panel). The apoB-100/apoB-48 levels were determined semiquantitatively using Bio-Rad Quantity One software (right panel).

mice with liver-specific perilipin 2 knockdown appeared creamy and turbid, whereas the control plasma was clear and bright (Fig. 4B). These data indicate that perilipin 2 is a negative regulator of VLDL-TAG secretion, and its knockdown completely rescues the VLDL-TAG secretion defect caused by *Cideb* deficiency.

To confirm that the increased TAG secretion is indeed due to increased VLDL lipidation and not to enhanced apoB synthesis and secretion, we measured the levels of hepatic apoB-100/apoB-48 and MTP, two proteins crucial for VLDL assembly, and observed no difference in their expression levels in *Cideb*$^{-/-}$ mice with liver-specific perilipin 2 knockdown compared with controls (Fig. 4C). In addition, the plasma levels of apoB were similar in *Cideb*$^{-/-}$ mice with or without perilipin 2 knockdown (Fig. 4D). Furthermore, the secretion rates of apoB-100 and apoB-48 were similar in *Cideb*$^{-/-}$ mice with or without perilipin 2 knockdown (Fig. 4E). Consistent with previous analysis in McA-RH7777 cells (32), the overexpression of perilipin 2 in the livers of wild-type mice increased hepatic TAG accumulation, reduced plasma TAG levels, and significantly decreased VLDL-TAG secretion (data not shown). Therefore, perilipin 2 is a negative regulator of VLDL lipidation, and its deficiency enhances VLDL lipidation and maturation in the livers of *Cideb*$^{-/-}$ mice.

Knockdown of perilipin 2 restores mature VLDL accumulation in the Golgi of *Cideb*$^{-/-}$ livers under fasting conditions

To provide further evidence that perilipin 2 knockdown in the livers of *Cideb*$^{-/-}$ mice leads to increased VLDL lipidation, we isolated the Golgi and ER microsomal fractions from the livers of *Cideb*$^{-/-}$ mice with or without perilipin 2 knockdown, and then separated the lipoproteins from the fractions by sucrose density gradient centrifugation. Under fasting conditions, lower levels of mature VLDL particles (densities ranging from 1.0 to 1.005) were detected in the Golgi microsomal fractions from the livers of *Cideb*$^{-/-}$ mice with control adenovirus (**Fig. 5A**). However, high levels of mature VLDL were observed in the Golgi fractions from the livers of *Cideb*$^{-/-}$ mice with liver-specific knockdown of perilipin 2 (Fig. 5A). In contrast, the ER fractions from the livers of *Cideb*$^{-/-}$ mice with or without perilipin 2 knockdown exhibited similar distributions of lipoprotein particles (Fig. 5B). Increased mature VLDL accumulation in the Golgi fraction (fraction 1) was also observed in wild-type mice with liver-specific knockdown of perilipin (supplementary Fig. II). These data indicate that, under fasting conditions, perilipin 2 is a negative regulator of VLDL lipidation. Under fed conditions, the amount of mature VLDL particles in the liver Golgi fractions and the levels of hepatic TAG were similar between wild-type and *Cideb*$^{-/-}$ mice with or without liver-specific knockdown of perilipin 2 (supplementary Fig. III). These data indicate that Cideb and perilipin 2 play specific roles in controlling hepatic TAG accumulation and VLDL lipidation under fasting conditions.

Perilipin 2 deficiency enhances LD size in *Cideb*$^{-/-}$ hepatocytes

Because both Cideb and perilipin 2 are LD-associated proteins, we further assessed the morphology of the LDs in

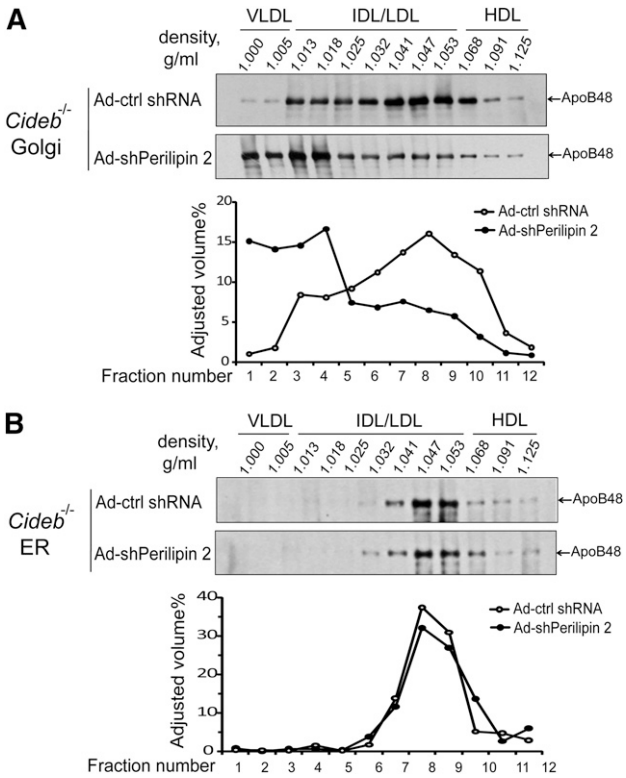

Fig. 5. Knockdown of perilipin 2 increases the levels of mature VLDL particles in the Golgi fractions from *Cideb*$^{-/-}$ livers. Density distribution of apoB-containing lipoproteins in the Golgi (A) and ER fractions (B) with or without perilipin 2 knockdown. ApoB-containing lipoproteins were isolated from the lumenal contents of the Golgi or ER fractions by sucrose density gradient centrifugation. ApoB was immunoprecipitated from each fraction, separated by SDS-PAGE, and assessed by fluorography. The labels at the top of the Western blots are the measured densities and show the expected distributions of the lipoproteins. The intensity of each band was estimated using Bio-Rad Quantity One software. The results shown are representative of two independent experiments. HDL, high-density lipoprotein; IDL/LDL, intermediate/low-density lipoprotein.

Cideb$^{-/-}$ hepatocytes with or without perilipin 2 knockdown. Consistent with the role of CIDE proteins in controlling LD size (51), *Cideb*$^{-/-}$ hepatocytes contained much smaller and more clustered LDs compared with wild-type cells (**Fig. 6A**). The accumulation of a large number of small LDs in *Cideb*$^{-/-}$ hepatocytes was further confirmed by electron microscopy (Fig. 6B). When perilipin 2 was knocked down in wild-type hepatocytes, the sizes of the LDs were increased (Fig. 6C). Statistical analysis revealed that the majority of the LDs in wild-type hepatocytes manifested sizes ranging 1–2 μm in diameter (Fig. 6D), with a small population (less than 2%) of LDs larger than 3 μm in diameter. However, more than 30% of the LDs in wild-type hepatocytes with perilipin 2 knockdown were larger than 3 μm in diameter (Fig. 6D). Knocking down perilipin 2 in *Cideb*$^{-/-}$ hepatocytes also significantly increased the LD size; more than 50% of LDs were 1–2 μm in diameter, whereas 65% of the LDs in *Cideb*$^{-/-}$ hepatocytes were less than 1 μm in diameter (Fig. 6E, F). These data indicate that Cideb and perilipin 2 also play opposing roles in controlling LD size, with Cideb as a positive and perilipin 2 as a negative regulator of LD size in hepatocytes.

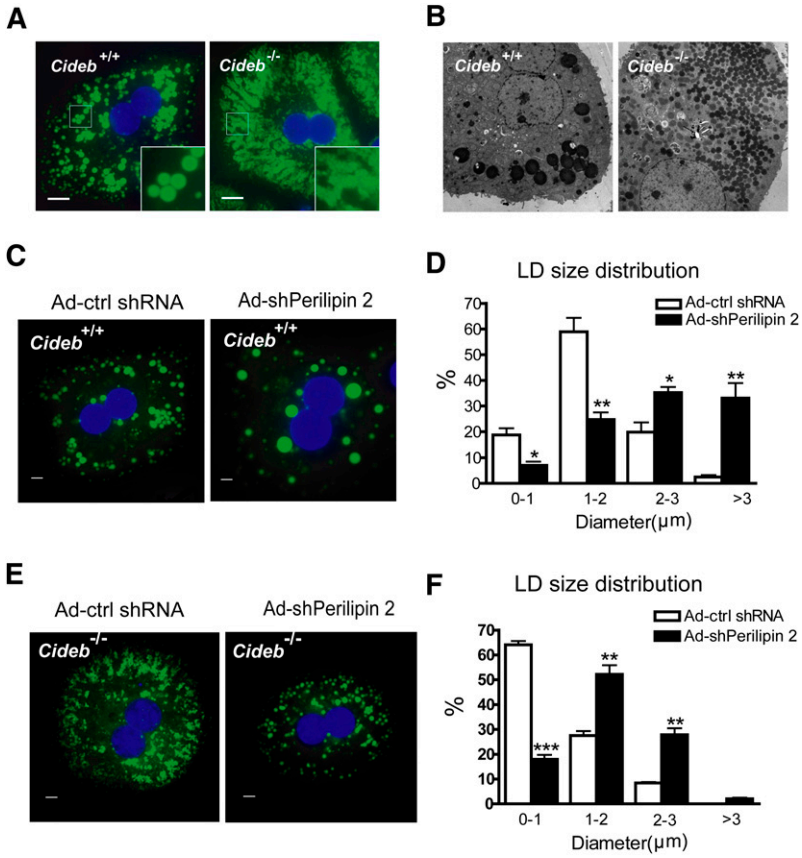

Fig. 6. *Cideb*$^{-/-}$ hepatocytes have smaller and more clustered LDs, and the knockdown of perilipin 2 increases the size of LDs. (A) Fluorescent microscopic images of hepatocytes isolated from wild-type or *Cideb*$^{-/-}$ mice and stained with Bodipy 493/503 (green). Scale bars, 10 μm. (B) EM images of hepatocytes isolated from wild-type and *Cideb*$^{-/-}$ mice. Scale bars, 10 μm. (C–F) Knockdown of perilipin 2 increases the LD size in wild-type (C, D) and *Cideb*$^{-/-}$ (E, F) hepatocytes. Wild-type and *Cideb*$^{-/-}$ mice were injected with adenoviruses containing Ad-shPerilipin 2 or Ad-ctrl shRNA (n = 5 each) for a week. Hepatocytes were isolated and incubated with 400 μM OA for 12 h before staining. The LDs were stained with Bodipy 493/503 (green). Fluorescent microscope images (C, E) and statistical analysis (D, F) showing the LD size distribution. Scale bars, 5 μm. *$P < 0.05$, **$P < 0.01$, ***$P < 0.001$. Data are the means ± SEM.

DISCUSSION

One long-standing question about VLDL assembly and maturation is how cytosolic TAG is transferred from the lipid storage organelles, LDs, to pre-VLDL particles. We have previously shown that Cideb is localized to the LDs and ER, and hepatocytes with *Cideb* deficiency exhibited increased TAG accumulation under fasting conditions and reduced VLDL-TAG secretion (47). Here, we demonstrate that Cideb is also detected in the Golgi apparatus, an important site for VLDL lipidation and maturation. *Cideb*$^{-/-}$ mice exhibited significantly reduced accumulation of mature VLDL particles in the Golgi fractions from the liver. Interestingly, we observed that the expression of perilipin 2, a LD-associated protein, is markedly upregulated in the livers of *Cideb*$^{-/-}$ mice. Knocking down perilipin 2 in the livers of *Cideb*$^{-/-}$ mice restored VLDL lipidation, increased VLDL-TAG secretion, and decreased hepatic lipid storage in *Cideb*$^{-/-}$ mice. Consistent with the role of CIDE proteins in promoting LD growth, *Cideb*$^{-/-}$ hepatocytes accumulate small LDs. Interestingly, *perilipin 2* deficiency in both wild-type and *Cideb*$^{-/-}$ hepatocytes resulted in the accumulation of larger LDs.

Cideb has been previously shown to localize to the LDs and ER by fluorescent staining and biochemical fractionation, similar to Cidea and Fsp27 (43, 44, 47, 52, 53). Here, using a sucrose density gradient centrifugation approach, we observed that Cideb is also localized to the Golgi apparatus. The localization of Cideb to three subcellular compartments (LDs, ER, and Golgi) is a unique feature, as using similar approaches demonstrated that perilipin 2 is specifically localized to LDs but not to the ER or Golgi. Furthermore, other ER-associated proteins (MTP and GRP94) are not associated with the Golgi or LDs. The broad distribution of Cideb in the ER and Golgi apparatus overlaps with apoB, providing a physical basis for its role in interacting with apoB and controlling VLDL lipidation.

Based on our previous and current analyses, Cideb appears to be an important positive regulator of VLDL lipidation and maturation in the livers as *Cideb*$^{-/-}$ mice. In addition, isolated *Cideb*$^{-/-}$ hepatocytes exhibit reduced VLDL lipidation and TAG secretion. In contrast, the overexpression of Cideb in the livers of *Cideb*$^{-/-}$ mice increases VLDL lipidation and TAG secretion (47). Furthermore, Cideb has been shown to mediate PGC-1α-stimulated VLDL-TAG secretion in HepG2 cells (54). Finally, we demonstrate here that the Golgi fractions in the livers of *Cideb*$^{-/-}$ mice contain significantly reduced levels of mature VLDL. What is the molecular mechanism of Cideb-mediated LD growth and VLDL lipidation? Cidea and Fsp27, two proteins highly related to Cideb, are clustered and enriched at LD contact sites (LDCS) and promote lipid transfer and LD growth (51). By analogy, Cideb may promote VLDL lipidation through its interaction with apoB and direct the transfer of TAG from cytosolic LDs to pre-VLDL particles that are anchored to the membrane of the ER and/or Golgi apparatus. Alternatively, Cidea and Fsp27 have been reported to control LD size and lipid storage by regulating lipolysis in adipocytes, as *Fsp27* and *Cidea* deficiencies result in increased lipolysis (41, 43, 55),

whereas the overexpression of Cidea and Fsp27 leads to reduced lipolysis (52, 56–59). It is possible that Cideb-mediated VLDL lipidation is due to its role in regulating lipolysis and reesterification in hepatocytes.

Interestingly, we observed dramatically increased perilipin 2 expression in the livers of *Cideb*$^{-/-}$ mice. Perilipin 2 has been shown to be a negative regulator of hepatic microsomal TAG accumulation and VLDL secretion (32, 34, 35, 60). We have demonstrated that the depletion of perilipin 2 in the livers of *Cideb*$^{-/-}$ mice results in significantly decreased hepatic TAG accumulation and increased levels of VLDL-TAG secretion, reversing the phenotype caused by *Cideb* deficiency. Reducing the expression of perilipin 2 in the livers of *Cideb*$^{-/-}$ mice also restores VLDL lipidation, as the amount of mature VLDL particles accumulated in the Golgi apparatus of *Cideb*$^{-/-}$ hepatocytes is markedly increased. Unlike Cideb, which is localized to the LD, ER, and Golgi apparatus, perilipin 2 is specifically localized to the LDs but not to the ER or Golgi. How does a LD-associated protein like perilipin 2 control VLDL lipidation, which occurs in the ER or Golgi apparatus? Furthermore, how do we explain the increased VLDL lipidation in the absence of both positive (Cideb) and negative (perilipin 2) regulators? In addition to associating with LDs, perilipin 2 is found clustered at the cytoplasmic leaflets of the ER membrane next to the LDs (61), and reduced perilipin 2 expression causes the apposition of LDs and the ER membranes (23). In addition, apoB processing and LD formation have been shown to be closely connected, as LDs can be trapped in the ER membrane by binding to lipidated apoB (24). Cideb may act as a positive factor to bring cytosolic LDs into close proximity with pre-VLDL particles associated with ER and Golgi membranes to promote VLDL lipidation. The presence of perilipin 2 on the LD surface may prevent this close contact between the cytosolic LDs and pre-VLDL particles (**Fig. 7**). Therefore, the loss of perilipin 2 results in the close apposition of LDs with the ER or Golgi membranes and enhanced VLDL lipidation in the hepatocytes of wild-type and *Cideb*$^{-/-}$ mice. Alternatively, Cideb and perilipin 2 may control VLDL lipidation through their cooperative regulation of the lipolysis and reesterification pathways. Interestingly, we observed drastically increased perilipin 5 levels in LD fractions of *Cideb*$^{-/-}$ mice that had a perilipin 2 knockdown, suggesting that perilipin 5 may provide a compensatory effect for the loss of perilipin 2 in controlling LD formation and VLDL lipidation. However, LDs lacking Cideb and perilipin 2 (but increased perilipin 5) in hepatocytes may not be compatible with cytoplasmic storage, and their TAG would need to be shuttled into the secretory pathway (ER and Golgi) in the form of lumenal LDs for use in the final steps of VLDL lipidation in the Golgi. Overall, our data demonstrate that Cideb and perilipin 2 exhibit opposing effects in controlling LD growth and VLDL lipidation in hepatocytes.

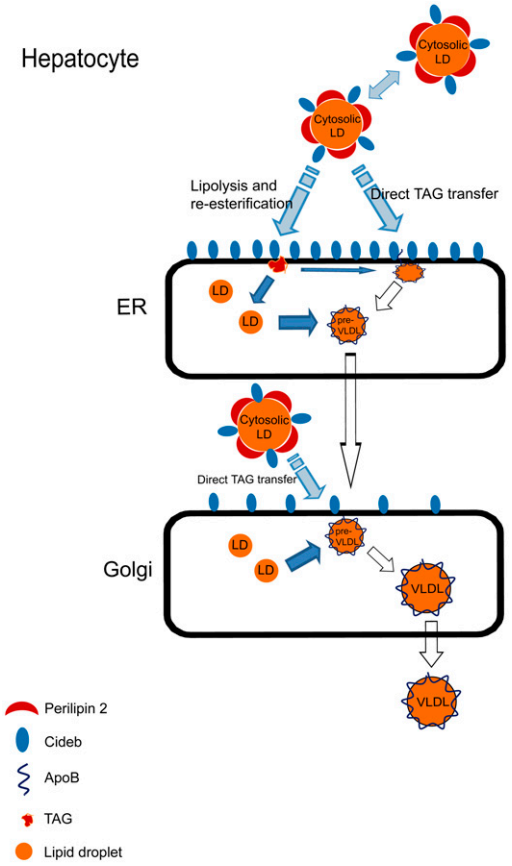

Fig. 7. Model of the possible functions of Cideb and perilipin 2 in regulating LD growth and VLDL lipidation. Cideb is localized to the Golgi, ER, and LDs. Perilipin 2 only localizes to LDs. Cideb may mediate VLDL lipidation in the ER or Golgi through the direct transportation of TAG from cytosolic LDs to pre-VLDL particles that are attached to the membrane of the ER and Golgi. Perilipin 2 may act as a physical barrier on LDs to block the Cideb-mediated close apposition of cytosolic LDs and pre-VLDL particles and inhibit the direct transportation of TAG from the LDs to pre-VLDL particles. Cideb and perilipin 2 may work cooperatively to regulate lipolysis and reesterification and control VLDL lipidation.

The authors thank the members of Peng Li's laboratory at Tsinghua University for helpful discussions and Dr. Ursula Andreo from the Departments of Medicine (Cardiology) and Cell Biology and the Marc and Ruti Bell Program in Vascular Biology, NYU School of Medicine, for technical assistance.

REFERENCES

1. Gibbons, G. F. 1990. Assembly and secretion of hepatic very-low-density lipoprotein. *Biochem. J.* **268:** 1–13.
2. Gibbons, G. F., D. Wiggins, A. M. Brown, and A. M. Hebbachi. 2004. Synthesis and function of hepatic very-low-density lipoprotein. *Biochem. Soc. Trans.* **32:** 59–64.
3. Rutledge, A. C., Q. Su, and K. Adeli. 2010. Apolipoprotein B100 biogenesis: a complex array of intracellular mechanisms regulating folding, stability, and lipoprotein assembly. *Biochem. Cell Biol.* **88:** 251–267.
4. Fisher, E. A., and H. N. Ginsberg. 2002. Complexity in the secretory pathway: the assembly and secretion of apolipoprotein B-containing lipoproteins. *J. Biol. Chem.* **277:** 17377–17380.
5. Olofsson, S. O., P. Stillemark-Billton, and L. Asp. 2000. Intracellular assembly of VLDL: two major steps in separate cell compartments. *Trends Cardiovasc. Med.* **10:** 338–345.
6. Yamaguchi, J., M. V. Gamble, D. Conlon, J. S. Liang, and H. N. Ginsberg. 2003. The conversion of apoB100 low density lipoprotein/high density lipoprotein particles to apoB100 very low density lipoproteins in response to oleic acid occurs in the endoplasmic reticulum and not in the Golgi in McA RH7777 cells. *J. Biol. Chem.* **278:** 42643–42651.

7. Alexander, C. A., R. L. Hamilton, and R. J. Havel. 1976. Subcellular localization of B apoprotein of plasma lipoproteins in rat liver. *J. Cell Biol.* **69:** 241–263.
8. Bamberger, M. J., and M. D. Lane. 1990. Possible role of the Golgi apparatus in the assembly of very low density lipoprotein. *Proc. Natl. Acad. Sci. USA.* **87:** 2390–2394.
9. Gusarova, V., J. Seo, M. L. Sullivan, S. C. Watkins, J. L. Brodsky, and E. A. Fisher. 2007. Golgi-associated maturation of very low density lipoproteins involves conformational changes in apolipoprotein B, but is not dependent on apolipoprotein E. *J. Biol. Chem.* **282:** 19453–19462.
10. Blasiole, D. A., A. T. Oler, and A. D. Attie. 2008. Regulation of ApoB secretion by the low density lipoprotein receptor requires exit from the endoplasmic reticulum and interaction with ApoE or ApoB. *J. Biol. Chem.* **283:** 11374–11381.
11. Gusarova, V., J. L. Brodsky, and E. A. Fisher. 2003. Apolipoprotein B100 exit from the endoplasmic reticulum (ER) is COPII-dependent, and its lipidation to very low density lipoprotein occurs post-ER. *J. Biol. Chem.* **278:** 48051–48058.
12. Tran, K., G. Thorne-Tjomsland, C. J. DeLong, Z. Cui, J. Shan, L. Burton, J. C. Jamieson, and Z. Yao. 2002. Intracellular assembly of very low density lipoproteins containing apolipoprotein B100 in rat hepatoma McA-RH7777 cells. *J. Biol. Chem.* **277:** 31187–31200.
13. Pan, M., J. S. Liang Js, E. A. Fisher, and H. N. Ginsberg. 2002. The late addition of core lipids to nascent apolipoprotein B100, resulting in the assembly and secretion of triglyceride-rich lipoproteins, is independent of both microsomal triglyceride transfer protein activity and new triglyceride synthesis. *J. Biol. Chem.* **277:** 4413–4421.
14. Olofsson, S. O., P. Bostrom, L. Andersson, M. Rutberg, J. Perman, and J. Boren. 2009. Lipid droplets as dynamic organelles connecting storage and efflux of lipids. *Biochim. Biophys. Acta.* **1791:** 448–458.
15. Farese, R. V., Jr., and T. C. Walther. 2009. Lipid droplets finally get a little R-E-S-P-E-C-T. *Cell.* **139:** 855–860.
16. Miyanari, Y., K. Atsuzawa, N. Usuda, K. Watashi, T. Hishiki, M. Zayas, R. Bartenschlager, T. Wakita, M. Hijikata, and K. Shimotohno. 2007. The lipid droplet is an important organelle for hepatitis C virus production. *Nat. Cell Biol.* **9:** 1089–1097.
17. Fukasawa, M. 2010. Cellular lipid droplets and hepatitis C virus life cycle. *Biol. Pharm. Bull.* **33:** 355–359.
18. Bell, M., H. Wang, H. Chen, J. C. McLenithan, D. W. Gong, R. Z. Yang, D. Yu, S. K. Fried, M. J. Quon, C. Londos, et al. 2008. Consequences of lipid droplet coat protein downregulation in liver cells: abnormal lipid droplet metabolism and induction of insulin resistance. *Diabetes.* **57:** 2037–2045.
19. Meex, R. C., P. Schrauwen, and M. K. Hesselink. 2009. Modulation of myocellular fat stores: lipid droplet dynamics in health and disease. *Am. J. Physiol. Regul. Integr. Comp. Physiol.* **297:** R913–R924.
20. Lungu, A. O., E. Safar Zadeh, A. Goodling, E. Cochran, and P. Gorden. 2012. Insulin resistance is a sufficient basis for hyperandrogenism in lipodystrophic women with polycystic ovarian syndrome. *J. Clin. Endocrinol. Metab.* **97:** 563–567.
21. Hayashi, T., and T. P. Su. 2003. Sigma-1 receptors (sigma(1) binding sites) form raft-like microdomains and target lipid droplets on the endoplasmic reticulum: roles in endoplasmic reticulum lipid compartmentalization and export. *J. Pharmacol. Exp. Ther.* **306:** 718–725.
22. Wang, H., D. Gilham, and R. Lehner. 2007. Proteomic and lipid characterization of apolipoprotein B-free luminal lipid droplets from mouse liver microsomes: implications for very low density lipoprotein assembly. *J. Biol. Chem.* **282:** 33218–33226.
23. Ozeki, S., J. Cheng, K. Tauchi-Sato, N. Hatano, H. Taniguchi, and T. Fujimoto. 2005. Rab18 localizes to lipid droplets and induces their close apposition to the endoplasmic reticulum-derived membrane. *J. Cell Sci.* **118:** 2601–2611.
24. Ohsaki, Y., J. Cheng, M. Suzuki, A. Fujita, and T. Fujimoto. 2008. Lipid droplets are arrested in the ER membrane by tight binding of lipidated apolipoprotein B-100. *J. Cell Sci.* **121:** 2415–2422.
25. Bar-On, H., P. S. Roheim, O. Stein, and Y. Stein. 1971. Contribution of floating fat triglyceride and of lecithin towards formation of secretory triglyceride in perfused rat liver. *Biochim. Biophys. Acta.* **248:** 1–11.
26. Francone, O. L., A. D. Kalopissis, and G. Griffaton. 1989. Contribution of cytoplasmic storage triacylglycerol to VLDL-triacylglycerol in isolated rat hepatocytes. *Biochim. Biophys. Acta.* **1002:** 28–36.
27. Wiggins, D., and G. F. Gibbons. 1992. The lipolysis/esterification cycle of hepatic triacylglycerol. Its role in the secretion of very-low-density lipoprotein and its response to hormones and sulphonylureas. *Biochem. J.* **284:** 457–462.
28. Gibbons, G. F., and D. Wiggins. 1995. Intracellular triacylglycerol lipase: its role in the assembly of hepatic very-low-density lipoprotein (VLDL). *Adv. Enzyme Regul.* **35:** 179–198.
29. Lankester, D. L., A. M. Brown, and V. A. Zammit. 1998. Use of cytosolic triacylglycerol hydrolysis products and of exogenous fatty acid for the synthesis of triacylglycerol secreted by cultured rat hepatocytes. *J. Lipid Res.* **39:** 1889–1895.
30. Dolinsky, V. W., D. N. Douglas, R. Lehner, and D. E. Vance. 2004. Regulation of the enzymes of hepatic microsomal triacylglycerol lipolysis and re-esterification by the glucocorticoid dexamethasone. *Biochem. J.* **378:** 967–974.
31. Bickel, P. E., J. T. Tansey, and M. A. Welte. 2009. PAT proteins, an ancient family of lipid droplet proteins that regulate cellular lipid stores. *Biochim. Biophys. Acta.* **1791:** 419–440.
32. Magnusson, B., L. Asp, P. Bostrom, M. Ruiz, P. Stillemark-Billton, D. Linden, J. Boren, and S. O. Olofsson. 2006. Adipocyte differentiation-related protein promotes fatty acid storage in cytosolic triglycerides and inhibits secretion of very low-density lipoproteins. *Arterioscler. Thromb. Vasc. Biol.* **26:** 1566–1571.
33. Imai, Y., G. M. Varela, M. B. Jackson, M. J. Graham, R. M. Crooke, and R. S. Ahima. 2007. Reduction of hepatosteatosis and lipid levels by an adipose differentiation-related protein antisense oligonucleotide. *Gastroenterology.* **132:** 1947–1954.
34. Chang, B. H., L. Li, A. Paul, S. Taniguchi, V. Nannegari, W. C. Heird, and L. Chan. 2006. Protection against fatty liver but normal adipogenesis in mice lacking adipose differentiation-related protein. *Mol. Cell. Biol.* **26:** 1063–1076.
35. Chang, B. H., L. Li, P. Saha, and L. Chan. 2010. Absence of adipose differentiation related protein upregulates hepatic VLDL secretion, relieves hepatosteatosis, and improves whole body insulin resistance in leptin-deficient mice. *J. Lipid Res.* **51:** 2132–2142.
36. Paul, A., B. H. Chang, L. Li, V. K. Yechoor, and L. Chan. 2008. Deficiency of adipose differentiation-related protein impairs foam cell formation and protects against atherosclerosis. *Circ. Res.* **102:** 1492–1501.
37. Listenberger, L. L., A. G. Ostermeyer-Fay, E. B. Goldberg, W. J. Brown, and D. A. Brown. 2007. Adipocyte differentiation-related protein reduces the lipid droplet association of adipose triglyceride lipase and slows triacylglycerol turnover. *J. Lipid Res.* **48:** 2751–2761.
38. Larigauderie, G., C. Cuaz-Perolin, A. B. Younes, C. Furman, C. Lasselin, C. Copin, M. Jaye, J. C. Fruchart, and M. Rouis. 2006. Adipophilin increases triglyceride storage in human macrophages by stimulation of biosynthesis and inhibition of beta-oxidation. *FEBS J.* **273:** 3498–3510.
39. Gong, J., Z. Sun, and P. Li. 2009. CIDE proteins and metabolic disorders. *Curr. Opin. Lipidol.* **20:** 121–126.
40. Yonezawa, T., R. Kurata, M. Kimura, and H. Inoko. 2011. Which CIDE are you on? Apoptosis and energy metabolism. *Mol. Biosyst.* **7:** 91–100.
41. Zhou, Z., S. Yon Toh, Z. Chen, K. Guo, C. P. Ng, S. Ponniah, S. C. Lin, W. Hong, and P. Li. 2003. Cidea-deficient mice have lean phenotype and are resistant to obesity. *Nat. Genet.* **35:** 49–56.
42. Zhou, L., L. Xu, J. Ye, D. Li, W. Wang, X. Li, L. Wu, H. Wang, F. Guan, and P. Li. 2012. Cidea promotes hepatic steatosis by sensing dietary fatty acids. *Hepatology.* Epub ahead of print. January 25, 2012; doi: 10.1002/hep.25611.
43. Toh, S. Y., J. Gong, G. Du, J. Z. Li, S. Yang, J. Ye, H. Yao, Y. Zhang, B. Xue, Q. Li, et al. 2008. Up-regulation of mitochondrial activity and acquirement of brown adipose tissue-like property in the white adipose tissue of fsp27 deficient mice. *PLoS ONE.* **3:** e2890.
44. Qi, J., J. Gong, T. Zhao, J. Zhao, P. Lam, J. Ye, J. Z. Li, J. Wu, H. M. Zhou, and P. Li. 2008. Downregulation of AMP-activated protein kinase by Cidea-mediated ubiquitination and degradation in brown adipose tissue. *EMBO J.* **27:** 1537–1548.
45. Li, J. Z., J. Ye, B. Xue, J. Qi, J. Zhang, Z. Zhou, Q. Li, Z. Wen, and P. Li. 2007. Cideb regulates diet-induced obesity, liver steatosis, and insulin sensitivity by controlling lipogenesis and fatty acid oxidation. *Diabetes.* **56:** 2523–2532.
46. Li, J. Z., Y. Lei, Y. Wang, Y. Zhang, J. Ye, X. Xia, X. Pan, and P. Li. 2010. Control of cholesterol biosynthesis, uptake and storage in hepatocytes by Cideb. *Biochim. Biophys. Acta.* **1801:** 577–586.

47. Ye, J., J. Z. Li, Y. Liu, X. Li, T. Yang, X. Ma, Q. Li, Z. Yao, and P. Li. 2009. Cideb, an ER- and lipid droplet-associated protein, mediates VLDL lipidation and maturation by interacting with apolipoprotein B. *Cell Metab.* **9:** 177–190.
48. Klaunig, J. E., P. J. Goldblatt, D. E. Hinton, M. M. Lipsky, J. Chacko, and B. F. Trump. 1981. Mouse liver cell culture. I. Hepatocyte isolation. *In Vitro.* **17:** 913–925.
49. Folch, J., M. Lees, and G. H. Sloane Stanley. 1957. A simple method for the isolation and purification of total lipides from animal tissues. *J. Biol. Chem.* **226:** 497–509.
50. Borensztajn, J., M. S. Rone, and T. J. Kotlar. 1976. The inhibition in vivo of lipoprotein lipase (clearing-factor lipase) activity by triton WR-1339. *Biochem. J.* **156:** 539–543.
51. Gong, J., Z. Sun, L. Wu, W. Xu, N. Schieber, D. Xu, G. Shui, H. Yang, R. G. Parton, and P. Li. 2011. Fsp27 promotes lipid droplet growth by lipid exchange and transfer at lipid droplet contact sites. *J. Cell Biol.* **195:** 953–963.
52. Puri, V., S. Ranjit, S. Konda, S. M. Nicoloro, J. Straubhaar, A. Chawla, M. Chouinard, C. Lin, A. Burkart, S. Corvera, et al. 2008. Cidea is associated with lipid droplets and insulin sensitivity in humans. *Proc. Natl. Acad. Sci. USA.* **105:** 7833–7838.
53. Nian, Z., Z. Sun, L. Yu, S. Y. Toh, J. Sang, and P. Li. 2010. Fat-specific protein 27 undergoes ubiquitin-dependent degradation regulated by triacylglycerol synthesis and lipid droplet formation. *J. Biol. Chem.* **285:** 9604–9615.
54. Chen, Z., J. Y. Norris, and B. N. Finck. 2010. Peroxisome proliferator-activated receptor-gamma coactivator-1alpha (PGC-1alpha) stimulates VLDL assembly through activation of cell death-inducing DFFA-like effector B (CideB). *J. Biol. Chem.* **285:** 25996–26004.
55. Nishino, N., Y. Tamori, S. Tateya, T. Kawaguchi, T. Shibakusa, W. Mizunoya, K. Inoue, R. Kitazawa, S. Kitazawa, Y. Matsuki, et al. 2008. FSP27 contributes to efficient energy storage in murine white adipocytes by promoting the formation of unilocular lipid droplets. *J. Clin. Invest.* **118:** 2808–2821.
56. Nordström, E. A., M. Ryden, E. C. Backlund, I. Dahlman, M. Kaaman, L. Blomqvist, B. Cannon, J. Nedergaard, and P. Arner. 2005. A human-specific role of cell death-inducing DFFA (DNA fragmentation factor-alpha)-like effector A (CIDEA) in adipocyte lipolysis and obesity. *Diabetes.* **54:** 1726–1734.
57. Puri, V., S. Konda, S. Ranjit, M. Aouadi, A. Chawla, M. Chouinard, A. Chakladar, and M. P. Czech. 2007. Fat-specific protein 27, a novel lipid droplet protein that enhances triglyceride storage. *J. Biol. Chem.* **282:** 34213–34218.
58. Christianson, J. L., E. Boutet, V. Puri, A. Chawla, and M. P. Czech. 2010. Identification of the lipid droplet targeting domain of the Cidea protein. *J. Lipid Res.* **51:** 3455–3462.
59. Ranjit, S., E. Boutet, P. Gandhi, M. Prot, Y. Tamori, A. Chawla, A. S. Greenberg, V. Puri, and M. P. Czech. 2011. Regulation of fat specific protein 27 by isoproterenol and TNF-alpha to control lipolysis in murine adipocytes. *J. Lipid Res.* **52:** 221–236.
60. Imamura, M., T. Inoguchi, S. Ikuyama, S. Taniguchi, K. Kobayashi, N. Nakashima, and H. Nawata. 2002. ADRP stimulates lipid accumulation and lipid droplet formation in murine fibroblasts. *Am. J. Physiol. Endocrinol. Metab.* **283:** E775–E783.
61. Robenek, H., O. Hofnagel, I. Buers, M. J. Robenek, D. Troyer, and N. J. Severs. 2006. Adipophilin-enriched domains in the ER membrane are sites of lipid droplet biogenesis. *J. Cell Sci.* **119:** 4215–4224.